

ESI

Chemo-chromism in an orthogonal dabco-based Co(II) network assembled by methanol-coordination and hydrogen bond formation

Misaki Shiga,^a Shogo Kawaguchi,^b Masaru Fujibayashi,^a Sadafumi Nishihara,^c Katsuya Inoue,^c Tomoyuki Akutagawa,^d Shin-ichiro Noro^f, Takayoshi Nakamura^e
and Ryo Tsunashima^{a, g*}

- a. *Graduate School of Sciences and Technology for Innovation, Yamaguchi University, Yoshida 1677-1, Yamaguchi, 753-8512, Japan.*
- b. *Japan Synchrotron Radiation Research Institute (JASRI), SPring-8, 1-1-1 Kouto, Sayo-cho, Sayo-gun, Hyogo 679-5198, Japan.*
- c. *Graduate School of Science, Hiroshima University, 1-3-1 Kagamiyama, Higashi-Hiroshima 739-8526, Japan.*
- d. *Institute of Multidisciplinary Research for Advanced Materials (IMRAM), Tohoku University, Sendai 980-8577, Japan.*
- e. *Research Institute for Electronic Science, Hokkaido University, Sapporo 001 0020, Japan.*
- f. *Faculty of Environmental Earth Science, Hokkaido University, Sapporo 060-0810, Japan*
- g. *Chemistry Course, Faculty of Science, Yamaguchi University, Yoshida 1677-1, Yamaguchi, 753-8512, Japan.*

1. Structural SC-XRD analysis
2. Magnetic measurement
3. P-XRD analysis
4. FTIR
5. UV-VIS-NIR spectra
6. NMR
7. GC-MS

1. Structural SC-XRD analysis

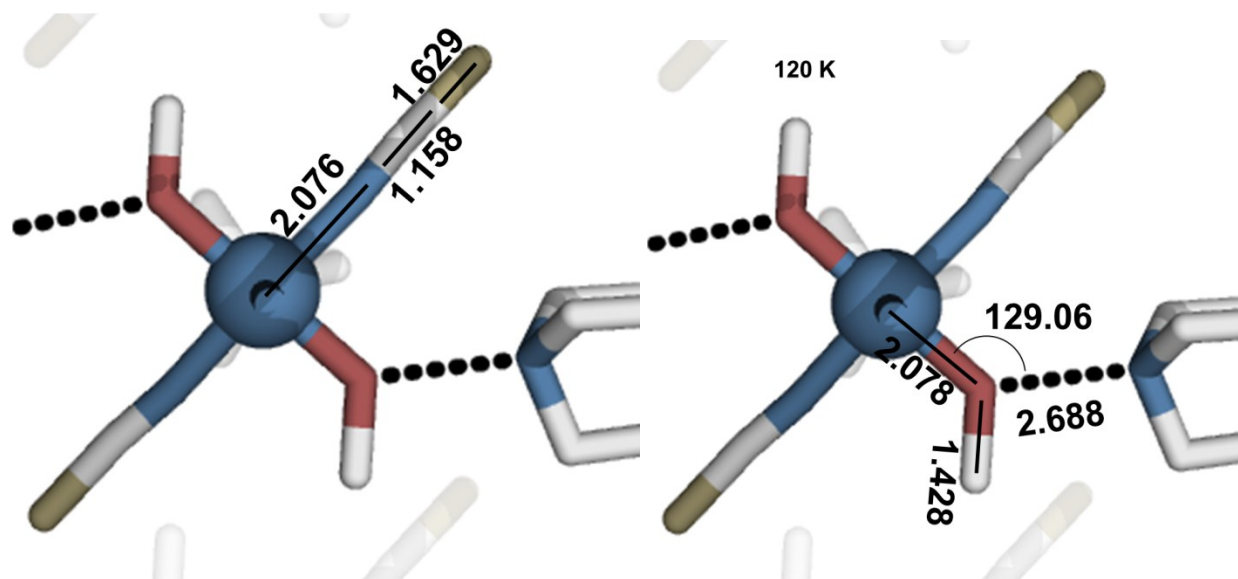


Figure S1-1. Bond and inter atomic distances in **1** for NCS ligand (left) and hydrogen bond (right) at 120 K.

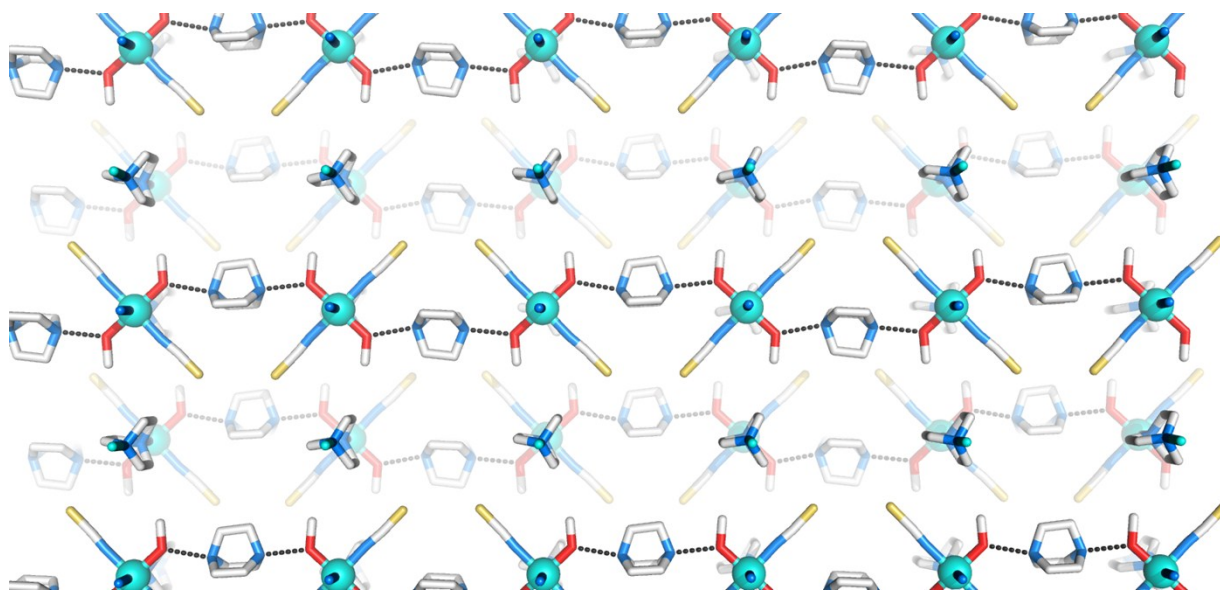


Figure S1-2. Crystal structure of **1-pink** (C: white, N: blue, O: red, S: yellow, Co: green) of *bc* plane. H-atoms and disordering of dabco(c) are omitted for clarifying illustrations.

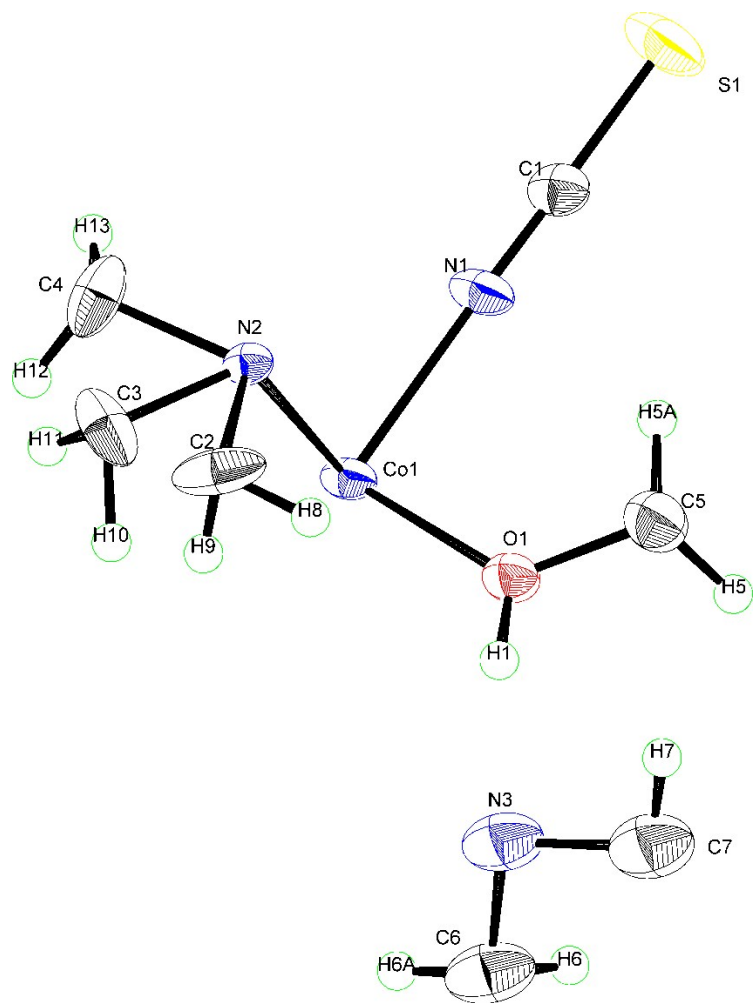


Figure S1-3. ORTEP view of structure

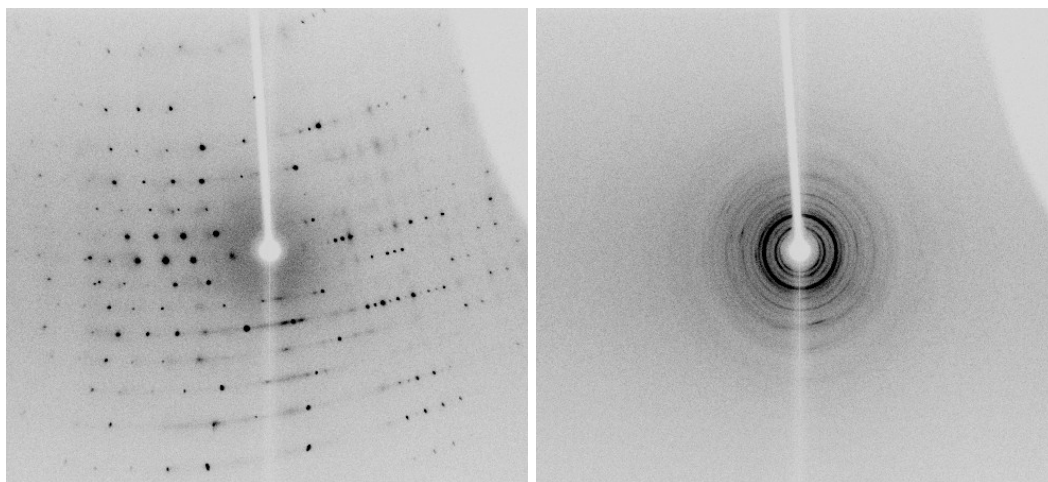


Figure S1-3. Diffraction patterns taken before (left) and after (right) incubation for 450 minutes at 90 degree using same single crystal with same angles (axis).

2. Magnetic measurement

Magnetic measurements were performed using a Quantum Design SQUID magnetometer. The temperature dependence of the molar magnetic susceptibility was measured between 2 and 350 K in an external field of 5,000 Oe. Powder samples were fixed in polyvinylidene chloride foils for measurements.

Line fitting was done by using MagSaki free soft* for a model of Co(II) mono-nuclear, axially distorted octahedral. Axial splitting parameter: Δ , spin-orbit coupling constant: λ (-172 cm^{-1} for Co(II)) and orbital reduction factor: κ were estimated to $\Delta = -533 \text{ cm}^{-1}$, $\lambda = -142 \text{ cm}^{-1}$, $\kappa = 0.75$. Further details on magnetic behaviour at the low temperature phase will be reported by us in elsewhere.

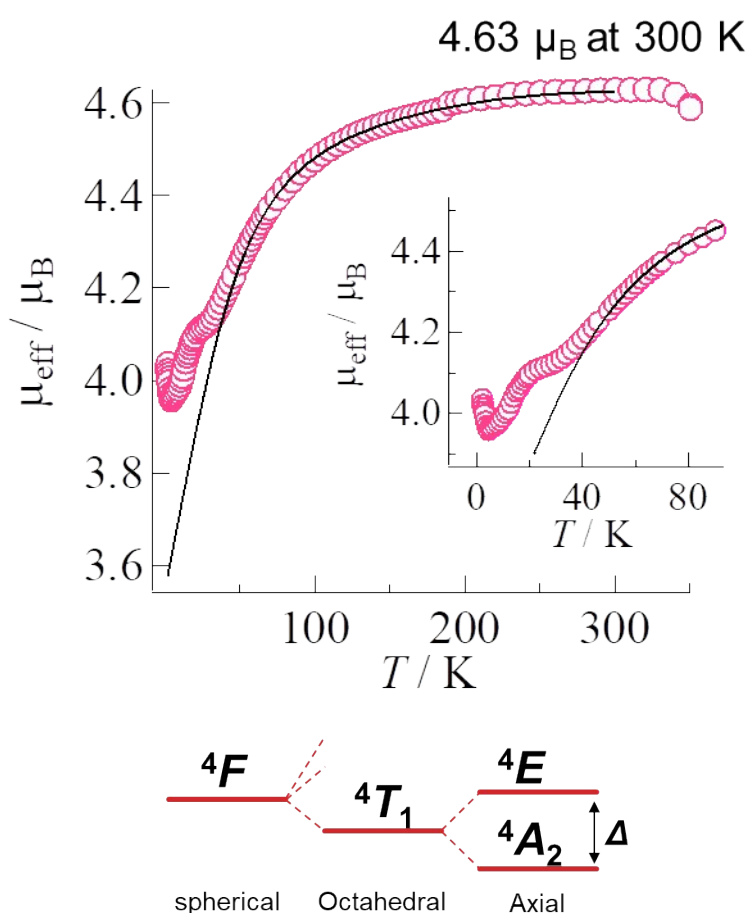


Figure S2-1. Temperature dependence of magnetic susceptibility (up) and scheme of electronic states (down).

*H. Sakiyama, *J. Chem. Software*, Vol.7, No.4, p.171–178(2001)

3. P-XRD analysis

Unit cell parameters of as grown and incubated sample (Figure S3-1 and -2) were estimated by Le Bail method (A. Le Bail, H. Duroy and J.L. Fourquet, Mat. Res. Bull. 23 (1988) 447-452.)

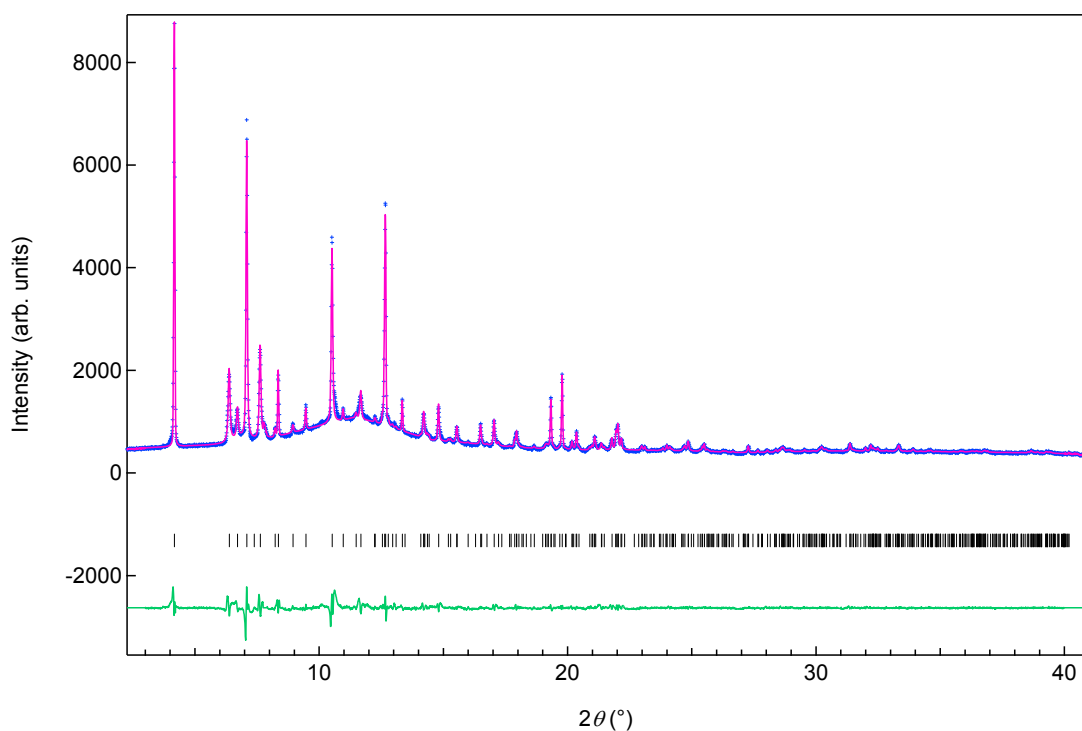


Figure S3-1. Whole pattern fitting of p-XRD pattern of as grown sample.

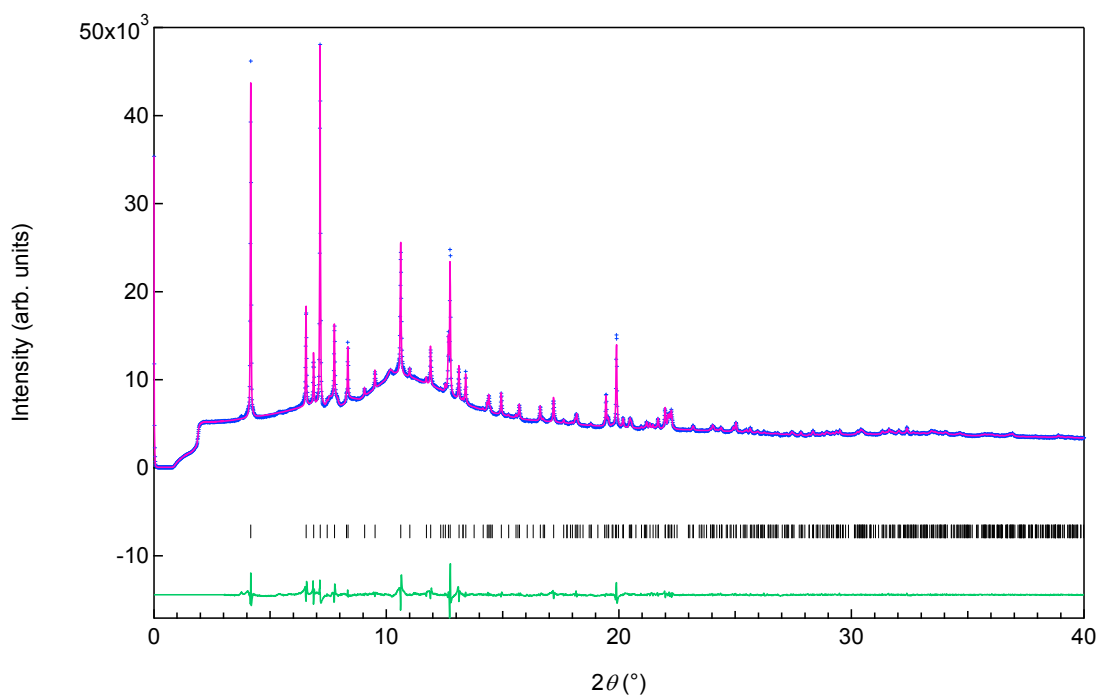


Figure S3-2. Whole pattern fitting of p-XRD pattern of sample after heating in vacuumed condition; (iv) in main text.

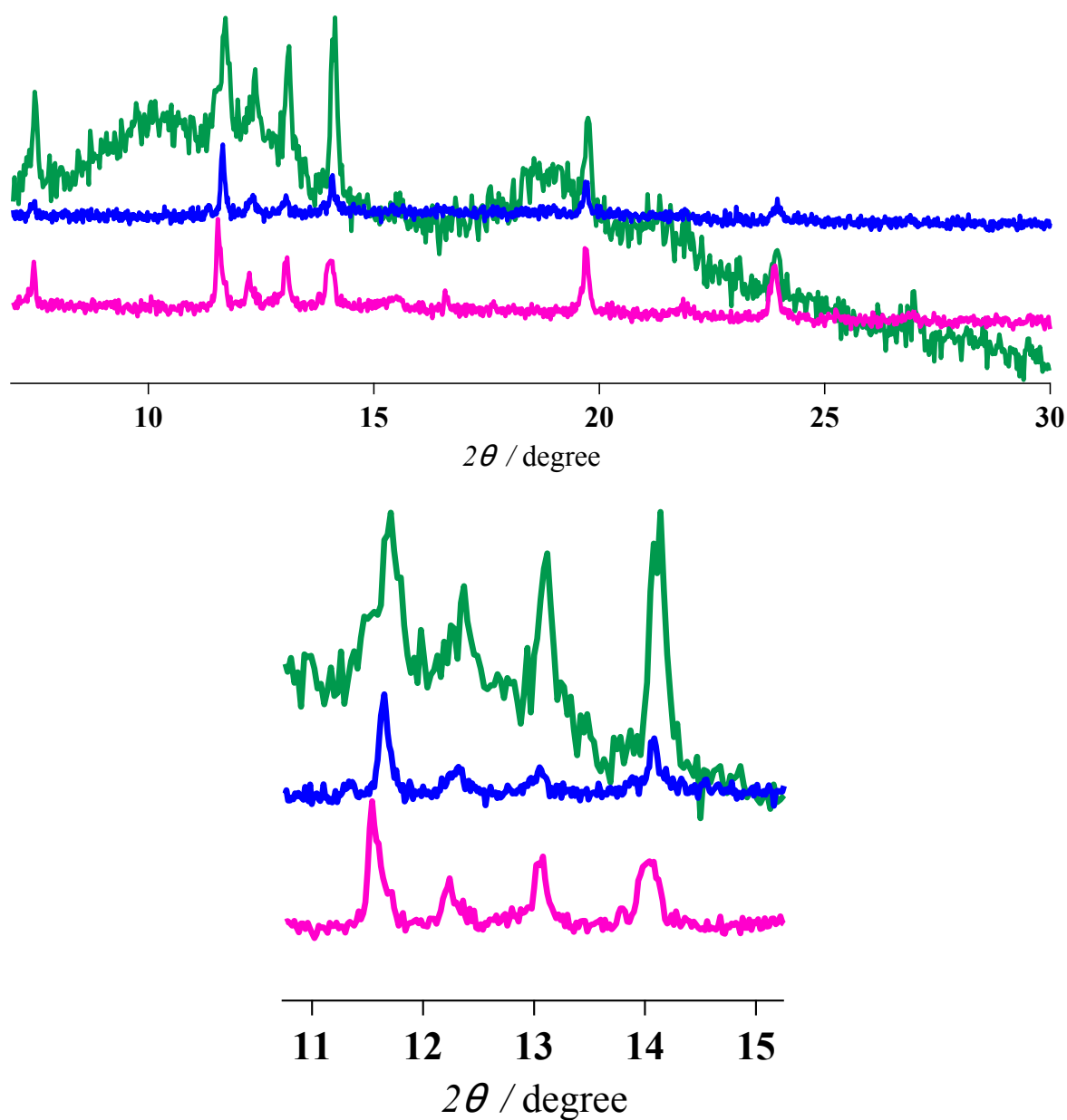


Figure S3-3. P-XRD of as-grown **1-pink** (pink), **1-blue** (blue) and sample after treating methanol to **1-blue** (green). Diffraction patterns were recoded using RIGAKU SmartLab.

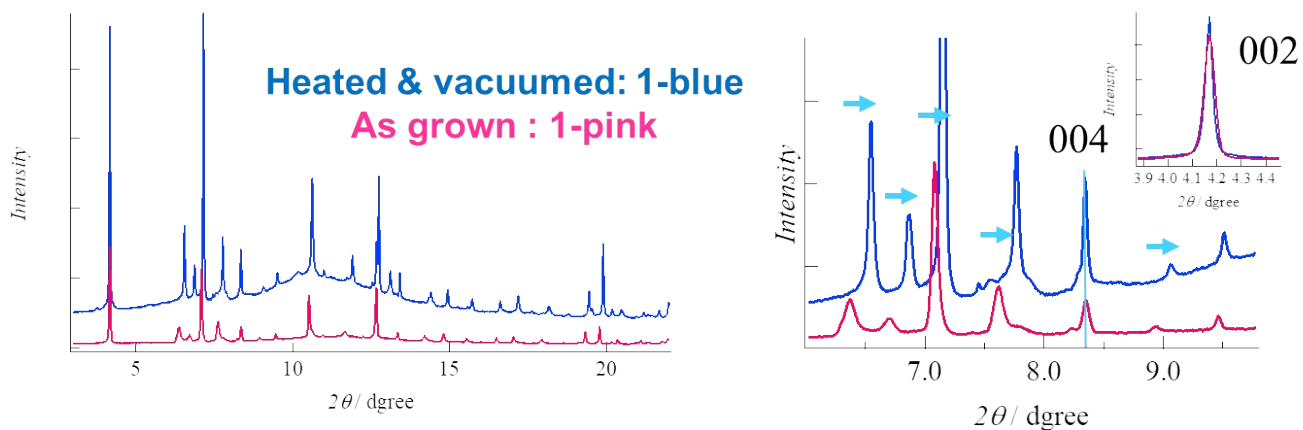


Figure S3-4. Comparison of powder pattern of as grown **1-pink** and **1-blue**.

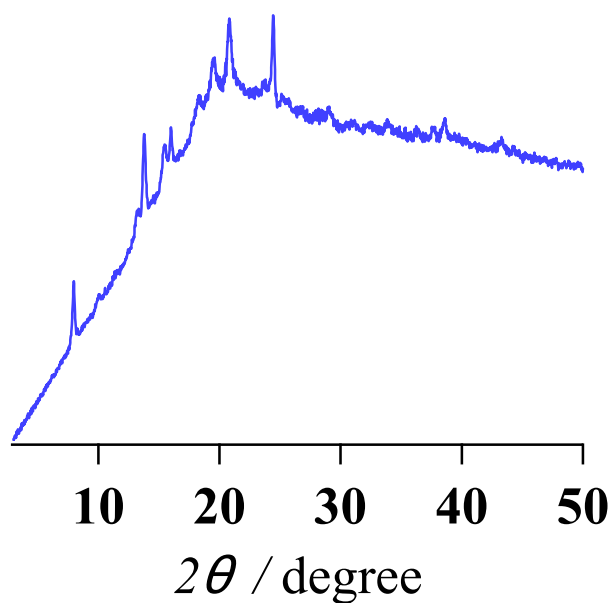


Figure S3-5. P-XRD of **1-pink** after grinding (**1-blue(a)**). Since peaks were observed, base line is appeared due to low intensities of diffractions.

4. FTIR

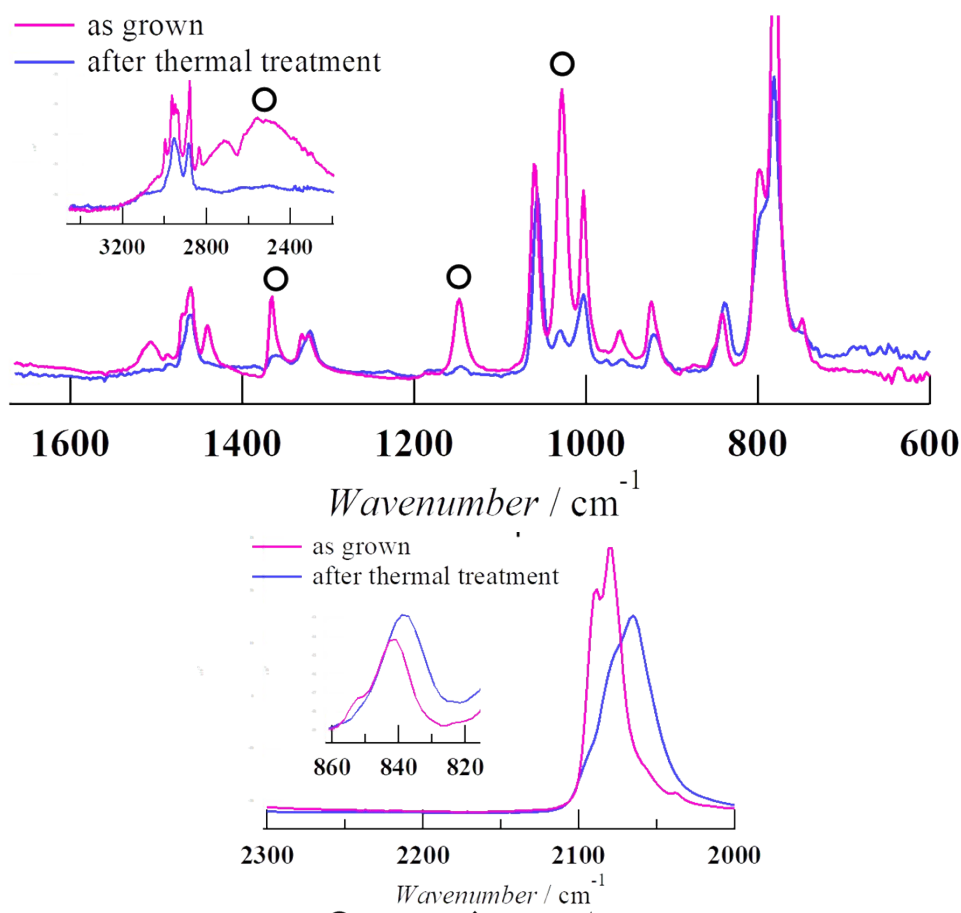


Figure S4-1. FTIR spectra of as-grown **1-blue** and after thermal treatment.

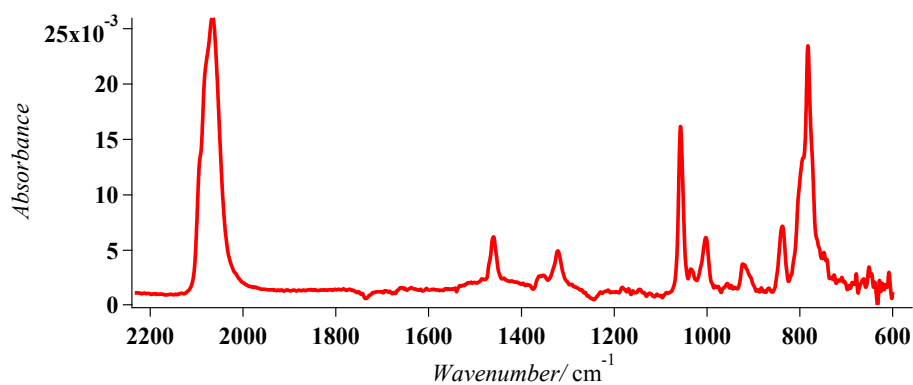


Figure S4-2. FT-IR spectra of well ground samples of **1-pink**.

Table S4-1. List of FTIR peak of NCS⁻ moiety

	1-pink	1-blue	>SCN	-NCS-	-SCN	-NCS
$\nu(\text{C-N})/\text{cm}^{-1}$	2079	2067	2200-2140	>2100	2130-2085	2100-2050
$\nu(\text{C-S})/\text{cm}^{-1}$	840	837		800-750	760-700	870-820

reference; Kabesova, M., & Gazo, J. (1980). *Chemicke Zvesti*, 34, 800–841.

5. UV-VIS-NIR spectra

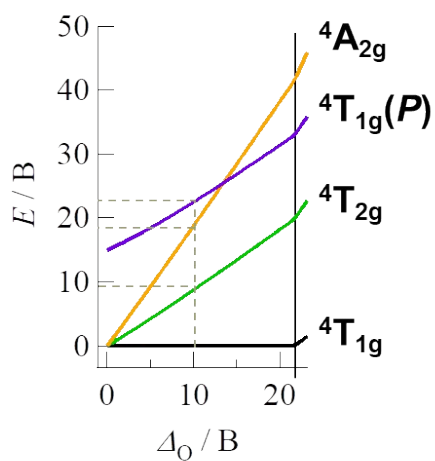
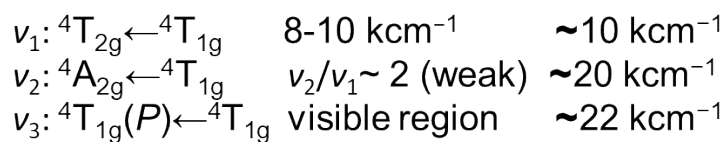
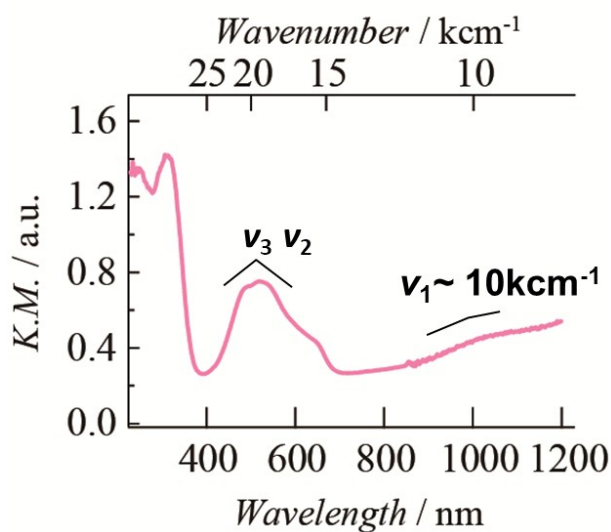


Figure S5-1. Diffusion-reflection spectra and peak assignments of **1-pink** with Tanabe-Sugano diagram.

A compound **1-blue(a)** was prepared by grading samples for 40 min and desorption of methanol was validated by IR measurement (Figure S4-2). P-XRD showed very weak intensity because of amorphous state (Figure S3-5). Treatments by methanol were performed by dropping 15 μL of methanol to **1-blue(a)** (0.01 g). Color of powder **1-blue(a)** was changed to pink by this methanol treatment. Spectra of **1-pink**, **1-blue** and **1-blue(a)** as well as **1-blue** and **1-blue (a)** after methanol treatments were shown in figure S5-2.

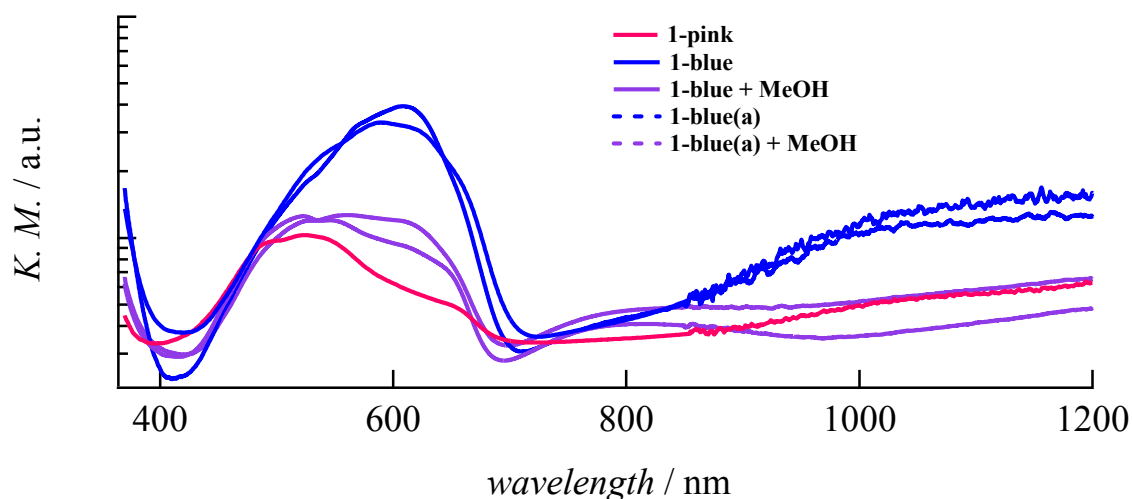


Figure S5-2. Diffusion-reflection spectra of compounds.

6. NRM

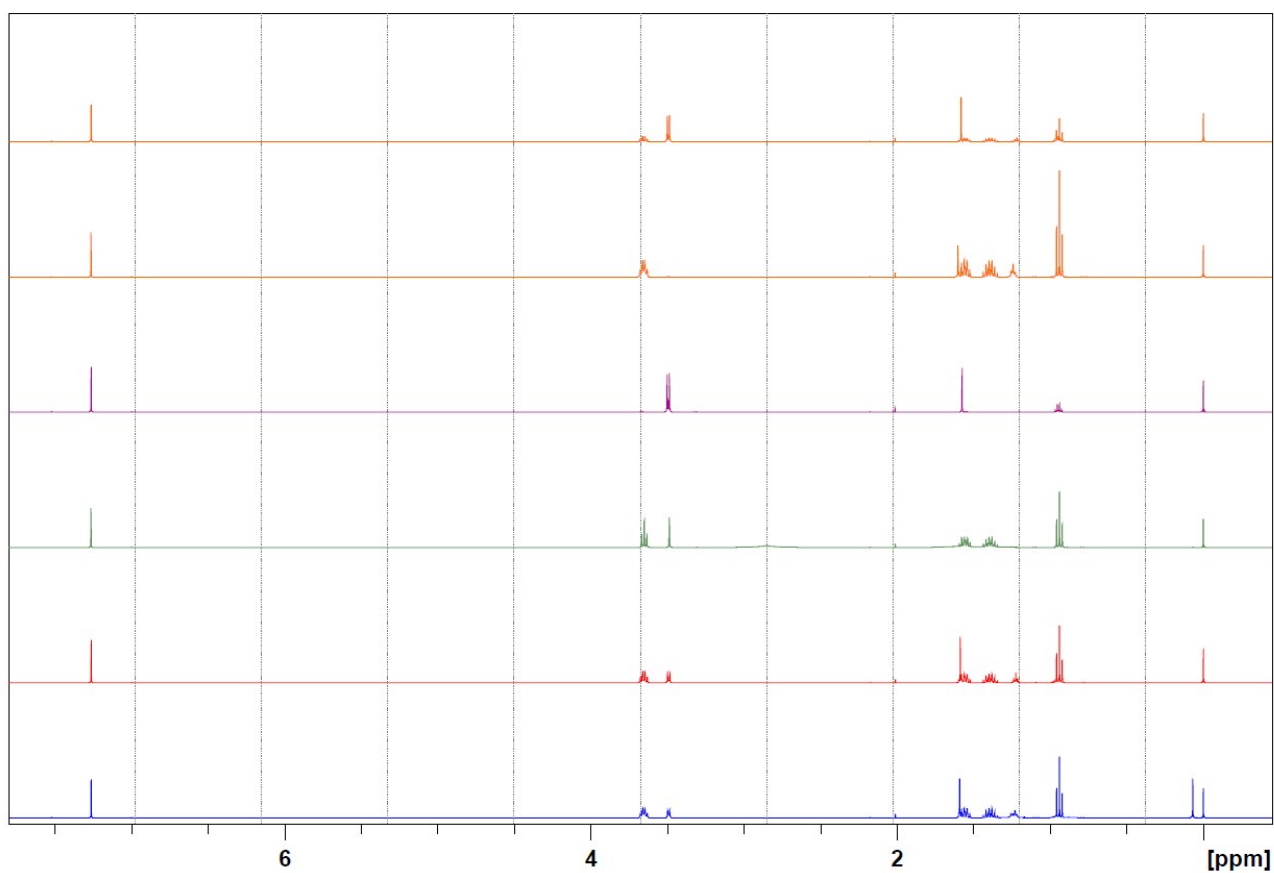


Figure S6-1. ¹H-NMR of chloroform solution of mixture of methanol and *n*-butanol, *n*-butanol, methanol, after treatment of **1-blue**, before treatment of **1-blue**, and controlled experiment with this order from up to down.

7. GC-MS

Time development of the GC-MS was characterized at 90 °C. Desorption of methanol was almost finished after 90 mints of incubation.

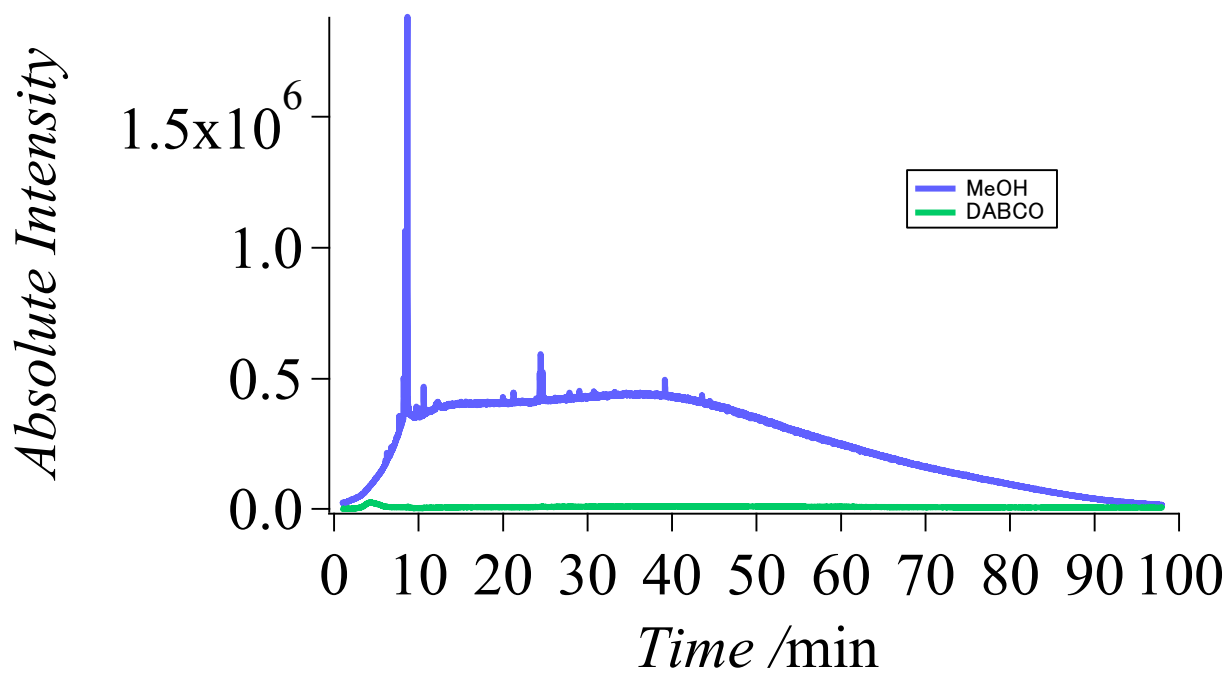


Figure S7-1. Time development of the GC-MS was characterized at 90 °C.